Nano-Confinement inside Molecular Metal Oxide Clusters: Dynamics and Modified Encapsulation Behavior

Zhe Wang,[a][d] Luke L. Daemen,[b] Yongqiang Cheng,[b] Eugene Mamontov,[b] Peter V. Bonnesen,[c] Kunlun Hong,[c] Anibal J. Ramirez-Cuesta,[b] and Panchao Yin*[a][b]

Abstract: Encapsulation behavior, as well as the presence of internal catalytically-active sites, has been spurring the applications of a 3 nm hollow spherical metal oxide cluster {Mo_{132}} as an encapsulation host and a nano-reactor. Due to its well-defined and tunable cluster structures, and nano-scaled internal void space comparable to the volumes of small molecules, this cluster provides a good model to study the dynamics of materials under Nano-confinement. Neutron scattering studies suggest that bulky internal ligands inside the cluster show slower and limited dynamics compared to their counterparts in the bulk state, revealing the rigid nature of the skeleton of the internal ligands. NMR studies indicate that the rigid internal ligands that partially cover the interfacial pore on the molybdenum oxide shells are able to block some large guest molecules from going inside the capsule cluster, which provides a convincing protocol for size-selective encapsulation and separation.

Thanks to recent developments in the design and construction of framework materials across multiple dimensions and length scales, the field of "materials under confinement" has been challenging and updating our knowledge in physics, chemistry, biology, and materials sciences.[1] Due to their close contact and nano-scaled/sub-nano-scaled sizes, the molecules under confinement show different dynamics in physical properties and higher reactivity and selectivity in their chemical properties compared to their counterparts in the bulk state.[1f, 1g, 2] Such concepts have been applied by chemists to build cage-shape clusters to catalyze chemical reactions with high reactivity, size selectivity, and region-selectivity.[3] In particular, molecular metal oxide clusters can provide both nano-confinement and catalytically-active centers for highly efficient and size-selective hydrolysis reactions.[3a, 3b] Due to the labile coordination of the bidentate ligands to metal centers on the internal surface of the clusters, the sizes of confinement, as well as the nature of internal surface, can be tuned by altering the internal surface ligands.[1d, 4] These modifications provide adaptability of the clusters to broad types of encapsulations and reactions.[5] When the size of the internal ligand becomes large, saturated occupation of the internal surface can be achieved through almost direct contact with their neighbors.[4c, 6] These ligands form a network that defines the pathway for the entrance of guest molecule.[4c, 6] The ligands could play decisive roles in regulating the entering/exiting of guest molecules besides the gating effect of the interfacial pores defined by metal oxide framework.[4d, 7] Therefore, the understanding of the dynamics of these ligands is critical both for cluster design, and for optimizing the ligand properties for target encapsulation and reactions.

Additionally, under the nano-confinement with size comparable to common molecules, limited numbers of molecules are encapsulated, and they are forced into close contact with their neighbors.[8] At the same time, the interfacial areas of the confined materials are high and therefore the interaction between these materials and the internal surface of the clusters would become a non-negligible factor in studying their properties.[9] The dynamics and chemical properties of 3D nano-confined materials are expected to be a new topic in fundamental physical and materials sciences.[10] Herein, quasielastic neutron scattering (QENS) and inelastic neutron scattering (INS) spectroscopies are applied to quantitatively probe the motions of internal ligands inside metal oxide clusters. Moreover, confirmed by NMR studies, the quantitative understanding of the dynamics of the confined ligand renders us the ability to modify the encapsulation behaviors of the clusters for hard size selection rules against guest molecules.

A typical structure of the metal oxide clusters can be described as a molybdenum oxide cluster (formula: $[Mo^{VI}_{72}Mo^{V}_{60}O_{372}(Ligand)_{30-x}(H_2O)_{72+2x}]^{(42-x)-}$; abbreviation, {$Mo_{132}$}) with outside and inside diameter as 3 and 2 nm, respectively.[8a] The internal surface can be functionalized maximally with 30 ligands *via* the coordination between ligands and the {Mo^{V}_{2}} units (red polyhedron in Figure 1).[8a] The clusters with butyric acid (formula: $[Mo^{VI}_{72}Mo^{V}_{60}O_{372}(C_3H_7COO)_{24}(H_2O)_{84}]^{36-}$; abbreviation, {$C_4Mo_{132}$}) and valeric acid (formula: $[Mo^{VI}_{72}Mo^{V}_{60}O_{372}(C_4H_9COO)_{24}(H_2O)_{84}]^{36-}$; abbreviation, {$C_5Mo_{132}$}) as internal ligands, respectively, are selected as models based on the following considerations: 1) the ligands are bulky and in close contact with their neighbors, as determined from structural analysis; and 2) the internal area has void space for possible encapsulation of guest molecules.[4c, 6] There are a total of 20 hexagonal pores with a diameter of ~ 0.8 nm on the cluster surface, which are partially covered by the internal ligands from the inside view. The entering of guest molecules through the pores into the center void space of the clusters would be highly dependent on their sizes and the flexibility of the alkane fragments of the internal ligands, as well as the expandability of the sizes of the inorganic pores.[3a, 4d]

[a] Dr. Z. Wang, Dr. P. Yin
Shull Wollan Center, Neutron Sciences Directorate
Oak Ridge National Laboratory
Oak Ridge, Tennessee 37831, United States
E-mail: yinp@ornl.gov
[b] Dr. L. L. Daemen, Dr. Y. Cheng, Dr. E. Mamontov, Dr. A. J. Ramirez-Cuesta, Dr. P. Yin
Chemical and Engineering Materials Division, Neutron Sciences Directorate
Oak Ridge National Laboratory
Oak Ridge, Tennessee 37831, United States
[c] Dr. P. V. Bonnesen, Dr. K. Hong
Center for Nanophase Materials Sciences
Oak Ridge National Laboratory
Oak Ridge, Tennessee 37831, United States
[d] Dr. Z. Wang
Biology and Soft Matter Division, Neutron Sciences Directorate
Oak Ridge National Laboratory
Oak Ridge, Tennessee 37831, United States

Supporting information for this article is given via a link at the end of the document.

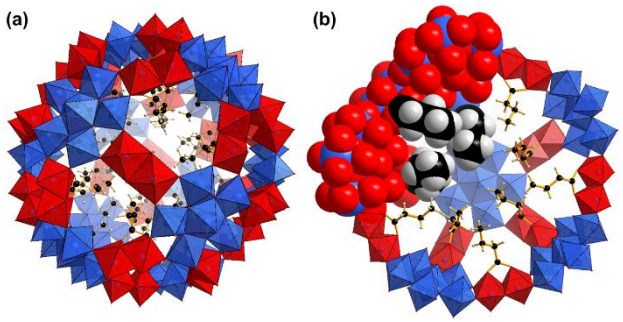

Figure 1. Polyhedron representation of the molecular structure of {C_4Mo_{132}}: a) the complete view and b) cross-sectional view (part of the structure is shown in space filling style in order to display the close contact of the internal ligands proportional to real atomic sizes). Color code for polyhedron: blue, $Mo^{VI}O_6$ or $Mo^{VI}O_7$; red, $Mo^{V}O_6$. Color code for spheres: black, C; grey, H.

QENS spectroscopy measurements were carried out to investigate the slow dynamics of the confined bulky ligands. In this technique, neutrons have a wavelength (4 to 12 Å) that is comparable to the inter-molecular distance of the materials. Therefore, QENS experiments are capable of providing a way for the measurement of the dynamic processes on a molecular length scale (*ca.* 1~20 Å) and microscopic time scale (*ca.* 1~10^4 ps).[11] Similar to the mechanism of dynamic light scattering, in a QENS experiment, momentum transfer $\boldsymbol{Q} = \boldsymbol{k}_\mathbf{f} - \boldsymbol{k}_\mathbf{i}$ and energy transfer $\hbar\omega = E_\mathrm{f} - E_\mathrm{i}$ of the neutron are measured. Here $\boldsymbol{k}_\mathbf{f}$ and $\boldsymbol{k}_\mathbf{i}$ are the wave vectors and E_f and E_i are energies of the scattered (final) and incident (initial) neutrons, respectively. Notice that the H atom has an exceptionally large incoherent scattering cross section compared to other elements, including Mo and O, the major elements comprising the cluster shell. Consequently, for materials containing a large number of H atoms, the neutron scattering spectrum is dominated by the incoherent scattering from H atoms.[11a] In this study, the measured spectrum is mainly contributed by the incoherent scattering from the H atoms on the internal ligands and thus reflects the individual motions of these confined alkane fragments.

A model that combines classical models of molecular translational, rotational and vibrational motions was used to interpret the QENS data. The model analysis will be able to provide the time and spatial parameters for each of these motions. By comparison with regular dynamics of non-confined molecules, the nano-confinement effect on the ligands can be clearly revealed from the analysis of the three motions. The details of the model fitting, and discussion of the QENS data, are listed as follows.

The QENS spectrum, $S_H(Q,\omega)$, is in a form of Fourier transform:[11a]

$$S_H(Q,\omega) = \frac{1}{2\pi}\int_{-\infty}^{+\infty} F_H(Q,t)e^{-i\omega t}dt, \quad (1)$$

The subscript "*H*" denotes that the QENS spectrum is a measurement of the incoherent scattering from the H atoms in the ligands. $F_H(Q,t)$ is called intermediate scattering function and is expressed as:[11a]

$$F_H(Q,t) = \frac{1}{N_H}\langle\sum_{l=1}^{N_H} e^{i\boldsymbol{Q}\cdot[\boldsymbol{r}_l(t)-\boldsymbol{r}_l(0)]}\rangle, \quad (2)$$

where N_H is the number of H atoms in the system, $\boldsymbol{r}_l(t)$ is the position vector of the *l*th H atom at time t, and $\langle\ldots\rangle$ represents the ensemble average of the system. From Eqs. (1) and (2) one can find that the functional form of $S_H(Q,\omega)$ is determined by the individual motion of the H atom ($\boldsymbol{r}_l(t) - \boldsymbol{r}_l(0)$). Thus it can give the dynamics of the ligands explicitly.

For our system, $F_H(Q,t)$ is modeled as a product of three contributions, namely, the vibrational part $F_V(Q,t)$, the translational part $F_T(Q,t)$, and the rotational part $F_R(Q,t)$, by assuming that these three motions are not significantly coupled:[12]

$$F_H(Q,t) \approx F_V(Q,t)F_T(Q,t)F_R(Q,t). \quad (3)$$

The vibrational part $F_V(Q,t)$ can be represented by the Debye-Waller factor $\exp(-Q^2\langle u^2\rangle/3)$, where $\langle u^2\rangle$ is the mean square displacement (msd) of the H atom.[11a] The translational motion of H atoms here is highly constrained in the hard inorganic cluster shell. The motion is also depressed by the coordination of ligands to the internal surface since the coordination bonds are statically and dynamically stable under the experimental conditions (295 K). Such kind of translational motion in a limited space is commonly modeled by a stretched exponential function plus a constant:[13]

$$F_T(Q,t) = A(Q) + [1 - A(Q)]\exp\left[-\left(\frac{t}{\tau_T(Q)}\right)^{\beta}\right], \quad (4)$$

where $\tau_T(Q)$ is the *Q*-dependent relaxation time of the translational motion and β is the stretching exponent. The constant $A(Q)$ can be used to evaluate the extent to what the translational motion is confined. It is equal to 0 for an unlimited translation and to 1 for the fixed particle.

Basically, $F_T(Q,t)$ represents the translational motion of skeleton of the alkyl chains, while $F_R(Q,t)$ reflects the rotation of the H atoms with respect to the corresponding C atom. We model $F_R(Q,t)$ as a rotational diffusion:[14]

$$F_R(Q,t) = \sum_{l=1}^{\infty}(2l+1)j_l(Qb)^2e^{-l(l+1)D_r t}, \quad (5)$$

where $j_l(x)$ is the *l*th-order spherical Bessel function, b is the radius of rotation, and D_r is the rotational diffusion coefficient defining how fast the rotational relaxation is. In this study, the first 4 terms in the right-hand-side of Eq. 5 are sufficient to describe the rotation. Notice that other models have been used to describe the rotations of H atoms in methyl groups and methylene group at high temperatures.[15] All these models have a form of exponential decay, and thus represent a stochastic process.

The measured QENS spectrum, $S_{H,m}(Q,\omega)$, is fitted by the theoretical spectrum $S_H(Q,\omega)$ convolved with the resolution function of the spectrometer to extract the 4 fitting parameters: $A(Q)$, $\tau_T(Q)$, β and D_r. The fitting quality is excellent for all measured spectra, as can be examined in Figure 2.

The QENS results for the {C_4Mo_{132}} sample are shown in Figure 3. Panel (a) gives a cartoon for the physical meanings of some important quantities in QENS analysis. Panel (b) gives the msd $\langle u^2\rangle$ as a function of temperature (*T*). At *T* < 150 K, msd is proportional to *T*, which is the feature of the harmonic solid. It shows that motion of the atoms at *T* < 150 K is no more than a vibration around equilibrium position. The msd undergoes a transition at T_c = 150 K. In previous studies on protein, a similar transition was observed at about 100 K and was ascribed to the activation of the methyl group rotation.[16] A higher T_c in our

sample indicates a stronger confinement effect compared with protein, which is usually considered as a densely packed liquid or glass. In addition, the deviation of msd from the linear extrapolation of the low-*T* data at $T > T_c$ is found to be quite weak. It suggests that at $T > T_c$, even some freedoms of motion are activated, but the overall motion of the ligand is still very constrained.

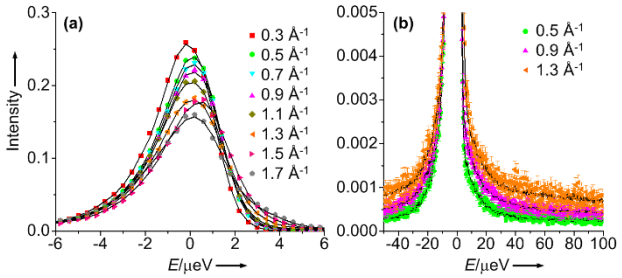

Figure 2. QENS spectra of $\{C_4Mo_{132}\}$ at 295 K for all the measured Q values. The measured spectra are represented by symbols and the fit curves are denoted by solid lines. Panel (a) shows the overall fitting quality and panel (b) examines the details of the fitting.

The parameter $A(Q)$ of the $\{C_4Mo_{132}\}$ sample is shown in Figure 3c. At first glance, all the values are close to 1, which suggests that the translational motion of the ligands is very restricted in space. For a translation in an impermeable sphere with a radius of *a*, $A(Q)$ has the following *Q*-dependence:[17]

$$A(Q) = [3j_1(Qa)/Qa]^2. \quad (6)$$

This equation allows a quantitative characterization of the confinement effect on the ligands. We fit $A(Q)$ of the $\{C_4Mo_{132}\}$ sample with Eq. (6) with the result also graphically presented in Figure 3c (the solid line). It gives $a = 0.508 \pm 0.021$ Å. This extremely small value directly shows the strong confinement effect on the ligands. Notice that, if we extrapolate the low-*T* ($T <$ 150 K) data of the msd to the room temperature (denoted by a dashed line in Figure 3b), the extrapolated value at 295 K, $\langle u_{ex}^2(295\ \mathrm{K})\rangle$, is 0.27 Å^2. It indicates a partial displacement of H atom of $\sim\sqrt{\langle u_{ex}^2(295\ \mathrm{K})\rangle} = 0.52$ Å. This part of the displacement is due to the vibration of the H atom around its equilibrium position, and is related to the displacement of the corresponding C atom. Its value is close to the confinement radius a, which shows that the major motion of the C atom in the skeleton is just the vibration around the equilibrium position. The conformational motions of the skeleton, such as the diffusion-like motion or the large-scale random walk, are substantially hindered in the equilibrium state. An alternative fit of the measured $A(Q)$ aimed at improving the fit quality is represented by the dashed line in Figure 3c. It can be obtained using the following equation:

$$A(Q) = C_{im} + (1 - C_{im})\left[\frac{3j_1(Qa)}{Qa}\right]^2. \quad (7)$$

Here C_{im} represents the contribution from the particles that do not participate in the spatially constrained translational motion. Such a fit gives a value of 0.90 for C_{im}, which indicates that the skeleton of the ligand is immobile. Thus, regardless of the model chosen, we can conclude that the conformation flexibility of the ligands is severely restricted.

Notice that, not all the nano-confining materials can exhibit such strong confinement effect on the translational motion of the confined ligand. Kintzel *et al.* found that, for the ligands confined in a nanoporous materials MCM-41 with diameter of several nanometers, effective diffusive motion can still be detected.[18] We assign the strong confinement effect in this study to the 3D confining geometry. In our case, both the head and the end of the confined ligand are restricted. The translational motion of the end is prohibited by the coordination bond to the shell, and the translational motion of the head is substantially constrained by the very close pack of the heads of all the ligands.

The total msd at 295 K, $\langle u^2(295\ \mathrm{K})\rangle$, is 0.49 Å^2, which indicates a displacement of H atom of $\sim\sqrt{\langle u^2(295\ \mathrm{K})\rangle} = 0.7$ Å. The excess part in $\langle u^2(295\ \mathrm{K})\rangle$ compared with $\langle u_{ex}^2(295\ \mathrm{K})\rangle$ is due to the rotation of H atom with respect to its corresponding C atom. The rotational diffusion coefficient D_r of the H atom in $\{C_4Mo_{132}\}$, extracted from the fit, is 1.1 ± 0.4 (10^8 s^{-1}). It corresponds to a time scale of $1/2D_r \approx 5$ ns. This time scale is larger than the typical time scale of the methyl group rotation in protein by at least one order of magnitude.[16] The slowing down of the rotation for the confined ligand is probably due to the strong interaction between the neighboring ligands. In fact, as shown in Figure 1b, the crowded distribution of the ligands inside the cluster and the curvature of the sphere lead to a significant interaction between the terminal methyl groups.[4c, 6]

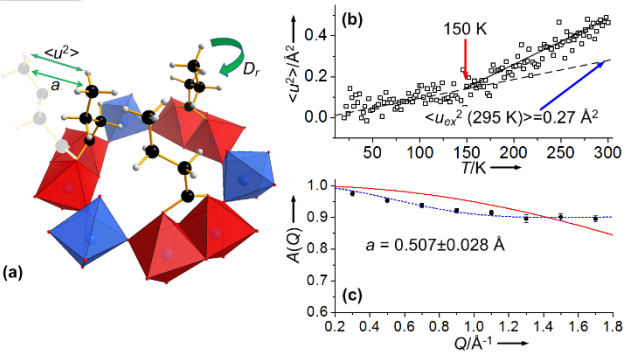

Figure 3. a) A cartoon for the physical meanings of the important quantities in the QENS analysis. $\langle u^2\rangle$ shows the displacement of the H atom in the time window of the QENS instrument, a gives the spatial range of the translational motion of the C atom, and D_r characterizes how fast the rotational relaxation of the methyl or methylene group; b) Mean square displacement (msd) of $\{C_4Mo_{132}\}$ as a function of *T*; c) $A(Q)$ for $\{C_4Mo_{132}\}$ at 295 K (solid squares) and the curve fitted with Eq. (6) (solid line). $A(Q) \gtrsim 0.9$ shows a very strong confinement effect on the translational motion of the constituent C atoms of the ligands. The dashed line represents another fit with Eq. (7).

The $\{C_5Mo_{132}\}$ sample was also studied under same experimental conditions in order to explore the possible effect of chain length to the dynamics of nano-confined ligands (see Figures S1 and S2 in supporting information). Given the fact that the confined space is defined by the rigid inorganic shell and these two clusters have an identical number of ligands inside them, the degree of close packing of the ligands is only determined by the sizes of their alkyl chain fragments.[4c, 6] Therefore, it is expected that the ligands (valeric acid) with longer backbones in $\{C_5Mo_{132}\}$ are more confined than that of

{C_4Mo_{132}} and thus their dynamics should be even slower. This is confirmed by a higher T_c and a slower rotational relaxation in the QENS results of {C_5Mo_{132}}: the transition temperature T_c is around 160 K and the rotational diffusion coefficient D_r is 0.5 ± 0.2 (10^8 s^{-1}), which corresponds to a time scale of $1/2D_r \approx 10$ ns.

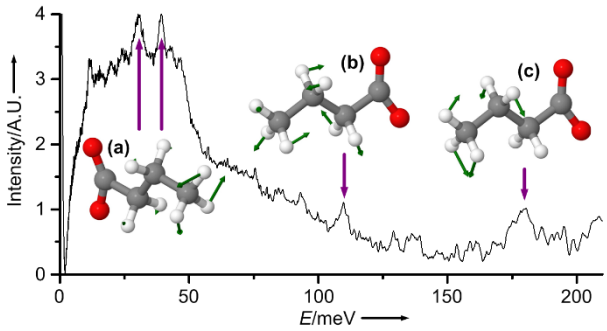

Figure 4. INS spectrum of {C_4Mo_{132}} at 10K and three different types of vibration modes of the butyric acid fragment.

INS measurements on these two samples were carried out in order to further explore the vibrational dynamics of confined ligands at high energy scales up to 400 meV. Compared to optic vibrational spectroscopic techniques, *e.g.*, IR and Raman spectroscopies, INS allows study of low-energy vibrations below ~25 meV and the detection of vibrations modes without hard selection rules.[19] More importantly, the neutron-proton incoherent scattering is dominant in the overall scattering signal, which greatly decreases the interference from the molybdenum oxide shell.[19] The peaks at energy lower than ~50 meV are ascribed as the torsion band of methyl and methylene groups. Specifically, based on theoretical simulation results, the two peaks at 30.7 and 39.3 meV originate from the torsion motion of terminal methyl groups of the internal ligands (vibrational mode (a) in Figure 4, see supporting information for more details). The peaks at higher energy correspond to bending modes of methyl groups or the coupling of bending modes and torsion modes. The sharp signal at 109.7 meV represents the coupling of bending mode and torsion mode (vibrational mode (b)) while the broad peak at 180.0 meV is contributed by a series of pure bending modes of the alkyl chain with tiny energy differences (vibrational mode (c)). The comparatively sharp appearance of most of the peaks is a strong confirmation of hindered vibration modes of the internal ligands and the confinement effect.

The encapsulation of a large guest molecule requires the collective thermal motion of the metal oxide pore structure and cooperative translational motion of the internal organic ligands.[3a, 4d, 5a] It is suggested from the above neutron studies that these bulky ligands are comparatively stiff with limited translational motion. It is, therefore, expected that some large molecules could be blocked out of the internal space of the cluster by the rigid ligands even though they can pass through the inorganic pores (Figure 5). In order to examine this scenario, ^{1}H-NMR was used to monitor the possible encapsulation of *n*-hexane and cyclohexane inside the {Mo_{132}} clusters with acetic acid as internal ligands (formula: $[Mo^{VI}_{72}Mo^{V}_{60}O_{372}(CH_3COO)_{30}(H_2O)_{72}]^{42-}$; abbreviation, {$C_2Mo_{132}$}) and {$C_4Mo_{132}$} in their aqueous solutions, respectively. It was indicated by the NMR results that both *n*-hexane and cyclohexane can be encapsulated inside {C_2Mo_{132}}, suggesting that the inorganic pores allow the entrance of these two alkanes (see Figure S3 in supporting information). However, only *n*-hexane can be encapsulated inside {C_4Mo_{132}} while no appearance of cyclohexane inside the cluster can be observed although the *ca.* 1 nm void spherical space at the center of {C_4Mo_{132}} is large enough for possible hosting of cyclohexane (Figure 5 and Figure S5 in supporting information). These studies imply that cyclohexane, with a larger cross section size as compared to *n*-hexane, is probably blocked out of the cluster by the butyric acid fragment matrix on the internal surface of the clusters. The NMR experiments confirm our assumption that the bulky internal ligands under nano-confinements have low tolerance of the sizes of the guest molecules.

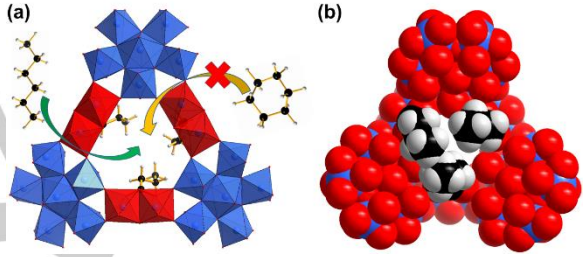

Figure 5. a) Polyhedron representation (view from outside of the cluster) and (b) space-filling model (view from inside the cluster) of the interfacial pore with internal ligands. Color code for polyhedron: blue, $Mo^{VI}O_6$ or $Mo^{VI}O_7$; red, $Mo^{V}O_6$. Color code for spheres: blue, Mo; black, C; grey, H.

The dynamics of internal bulky ligands inside {Mo_{132}} clusters has been explored by QENS and INS at different energy and time scales for the first time. Different from the soft nature of regular alkyl tails, the ligands under nano-confinement are found to be quite rigid, as suggested from their slow dynamics and limited diffusive motions and vibrations. The stiffness of these ligands modifies the encapsulation properties by displaying hard selection against the sizes of guest molecules. This work is instructive for the design of metal oxide clusters for encapsulation and catalysis purposes by revealing the importance of internal ligands. It also initiates the research on the materials properties under nano-confinement.

Acknowledgements

P. Y. is grateful to the support of Clifford G. Shull Fellowship from Neutron Sciences Directorate of Oak Ridge National Laboratory. The research performed in BL-2 (BASIS)[20] and BL-16B (VISION)[21] at ORNL's Spallation Neutron Source was sponsored by the Scientific User Facilities Division, Office of Basic Energy Sciences, U.S. Department of Energy. The sample preparation and NMR studies were conducted at the Center for Nanophase Materials Sciences, which is a DOE Office of

Science User Facility. Oak Ridge National Laboratory is supported by the Office of Science of the U.S. Department of Energy under Contract No. DE-AC05-00OR22725.

Keywords: polyoxometalte • confinement • dynamics • encapsulation • neutron scattering

[1] a) H.-C. Zhou, J. R. Long, O. M. Yaghi, *Chem. Rev.* **2012**, *112*, 673-674; b) B. M. Weckhuysen, J. Yu, *Chem. Soc. Rev.* **2015**, *44*, 7022-7024; c) Y. Wan, Zhao, *Chem. Rev.* **2007**, *107*, 2821-2860; d) A. Müller, P. Gouzerh, *Chem. Soc. Rev.* **2012**, *41*, 7431-7463; e) T. R. Cook, P. J. Stang, *Chem. Rev.* **2015**, *115*, 7001-7045; f) J. J. Kasianowicz, M. Kellermayer, D. DEAMER, *Structure and Dynamics of Confined Polymers: Proceedings of the NATO Advanced Research Workshop on Biological, Biophysical & Theoretical Aspects of Polymer Structure and Transport Bikal, Hungary 20–25 June 1999*, Springer Netherlands, **2002**; g) S. Cerveny, F. Mallamace, J. Swenson, M. Vogel, L. Xu, *Chem. Rev.* **2016,** Article ASAP, DOI: 10.1021/acs.chemrev.5b00609.

[2] a) E. E. Santiso, A. M. George, M. Sliwinska-bartkowiak, M. B. Nardelli, K. E. Gubbins, *Adsorption* **2005**, *11*, 349-354; b) D. Gentili, F. Valle, C. Albonetti, F. Liscio, M. Cavallini, *Acc. Chem. Res.* **2014**, *47*, 2692-2699; c) H.-X. Zhou, G. Rivas, A. P. Minton, *Annu. Rev. Biophys.* **2008**, *37*, 375-397.

[3] a) S. Kopilevich, A. Gil, M. Garcia-Ratés, J. Bonet-Ávalos, C. Bo, A. Müller, I. A. Weinstock, *J. Am. Chem. Soc.* **2012**, *134*, 13082-13088; b) S. Kopilevich, A. Müller, I. A. Weinstock, *J. Am. Chem. Soc.* **2015**, *137*, 12740-12743; c) Y. Inokuma, M. Kawano, M. Fujita, *Nature Chem.* **2011**, *3*, 349-358; d) M. Yoshizawa, J. K. Klosterman, M. Fujita, *Angew. Chem. Int. Ed.* **2009**, *48*, 3418-3438; e) T. Murase, S. Horiuchi, M. Fujita, *J. Am. Chem. Soc.* **2010**, *132*, 2866-2867; f) M. Yoshizawa, Y. Takeyama, T. Okano, M. Fujita, *J. Am. Chem. Soc.* **2003**, *125*, 3243-3247.

[4] a) A. Müller, E. Krickemeyer, H. Bögge, M. Schmidtmann, F. Peters, *Angew. Chem. Int. Ed.* **1998**, *37*, 3359-3363; b) O. Petina, D. Rehder, E. T. K. Haupt, A. Grego, I. A. Weinstock, A. Merca, H. Bögge, J. Szakács, A. Müller, *Angew. Chem. Int. Ed.* **2011**, *50*, 410-414; c) S. Garai, H. Bögge, A. Merca, O. A. Petina, A. Grego, P. Gouzerh, E. T. K. Haupt, I. A. Weinstock, A. Müller, *Angew. Chem. Int. Ed.* **2016**, *55*, 6634-6637; d) A. Ziv, A. Grego, S. Kopilevich, L. Zeiri, P. Miro, C. Bo, A. Müller, I. A. Weinstock, *J. Am. Chem. Soc.* **2009**, *131*, 6380-6382; e) A. Grego, A. Müller, I. A. Weinstock, *Angew. Chem. Int. Ed.* **2013**, *52*, 8358-8362.

[5] a) S. Kopilevich, H. Gottlieb, K. Keinan-Adamsky, A. Müller, I. A. Weinstock, *Angew. Chem. Int. Ed.* **2016**, *55*, 4476-4481; b) A. Müller, E. Krickemeyer, H. Bögge, M. Schmidtmann, B. Botar, M. O. Talismanova, *Angew. Chem. Int. Ed.* **2003**, *42*, 2085-2090; c) C. Schäffer, A. M. Todea, H. Bögge, O. A. Petina, D. Rehder, E. T. K. Haupt, A. Müller, *Chem. Eur. J.* **2011**, *17*, 9634-9639.

[6] C. Schäffer, H. Bögge, A. Merca, I. A. Weinstock, D. Rehder, E. T. K. Haupt, A. Müller, *Angew. Chem. Int. Ed.* **2009**, *48*, 8051-8056.

[7] A. Müller, Y. Zhou, H. Bögge, M. Schmidtmann, T. Mitra, E. T. K. Haupt, A. Berkle, *Angew. Chem. Int. Ed.* **2006**, *45*, 460-465.

[8] a) A. Müller, S. Roy, *Coord. Chem. Rev.* **2003**, *245*, 153-166; b) A. Mataz, B. M. Gregory, *J. Phys. Condens. Matter* **2005**, *17*, R461.

[9] a) A. Müller, S. Garai, C. Schäffer, A. Merca, H. Bögge, A. J. M. Al-Karawi, T. K. Prasad, *Chem. Eur. J.* **2014**, *20*, 6659-6664; b) T. Mitra, P. Miró, A.-R. Tomsa, A. Merca, H. Bögge, J. B. Ávalos, J. M. Poblet, C. Bo, A. Müller, *Chem. Eur. J.* **2009**, *15*, 1844-1852.

[10] P. Yin, B. Wu, E. Mamontov, L. L. Daemen, Y. Cheng, T. Li, S. Seifert, K. Hong, P. V. Bonnesen, J. K. Keum, A. J. Ramirez-Cuesta, *J. Am. Chem. Soc.* **2016**, *138*, 2638-2643.

[11] a) G. L. Squires, *Introduction to the Theory of Thermal Neutron Scattering*, Dover Publications, **1978**; b) S. H. Chen, M. Kotlarchyk, *Interaction of Photons and Neutrons with Matter: An Introduction*, World Scientific, **1997**; c) B. Wu, Y. Liu, X. Li, E. Mamontov, A. I. Kolesnikov, S. O. Diallo, C. Do, L. Porcar, K. Hong, S. C. Smith, L. Liu, G. S. Smith, T. Egami, W.-R. Chen, *J. Am. Chem. Soc.* **2013**, *135*, 5111-5117.

[12] a) J. Teixeira, M. C. Bellissent-Funel, S. H. Chen, A. J. Dianoux, *Phys. Rev. A* **1985**, *31*, 1913-1917; b) S. H. Chen, P. Gallo, F. Sciortino, P. Tartaglia, *Phys. Rev. E* **1997**, *56*, 4231-4243; c) F. Gabel, D. Bicout, U. Lehnert, M. Tehei, M. Weik, G. Zaccai, *Q. Rev. Biophys.* **2002**, *35*, 327-367.

[13] a) S. H. Chen, C. Liao, F. Sciortino, P. Gallo, P. Tartaglia, *Phys. Rev. E* **1999**, *59*, 6708-6714; b) Z. Wang, E. Fratini, M. Li, P. Le, E. Mamontov, P. Baglioni, S.-H. Chen, *Phys. Rev. E* **2014**, *90*, 042705.

[14] V. F. Sears, *Can. J. Phys.* **1967**, *45*, 237-254.

[15] M. Bée, *Quasielastic Neutron Scattering*, Adam Hilger, **1988**.

[16] J. H. Roh, V. N. Novikov, R. B. Gregory, J. E. Curtis, Z. Chowdhuri, A. P. Sokolov, *Phys. Rev. Lett.* **2005**, *95*, 038101.

[17] a) M. C. Bellissent-Funel, S. H. Chen, J. M. Zanotti, *Phys. Rev. E* **1995**, *51*, 4558-4569; b) F. Volino, A. J. Dianoux, *Mol. Phys.* **1980**, *41*, 271-279.

[18] E. J. Kintzel, M. K. Kidder, A. C. Buchanan, P. F. Britt, E. Mamontov, M. Zamponi, K. W. Herwig, *J. Phys. Chem. C* **2012**, *116*, 923-932.

[19] a) F. Barroso-Bujans, F. Fernandez-Alonso, J. A. Pomposo, S. Cerveny, A. Alegría, J. Colmenero, *ACS Macro Lett.* **2012**, *1*, 550-554; b) P. C. H. Mitchell, *Vibrational Spectroscopy with Neutrons: With Applications in Chemistry, Biology, Materials Science and Catalysis*, World Scientific, **2005**.

[20] E. Mamontov, K. W. Herwig, *Rev. Sci. Instrum.* **2011**, *82*, 085109.

[21] P. A. Seeger, L. L. Daemen, J. Z. Larese, *Nucl. Instr. Meth. Phys. Res.* **2009**, *604*, 719-728.

Table of Contents

COMMUNICATION

The dynamics of alkyl chains under nano-confinement inside a 3-nm nano-scaled molecular cluster was, for the first time, fully explored with neutron scattering techniques at different time- and energy- scales. The rigid nature of alkyl chains was revealed to be originated from their constrained motion under nano-confinement and further applied to tune the size-selective encapsulation behavior.

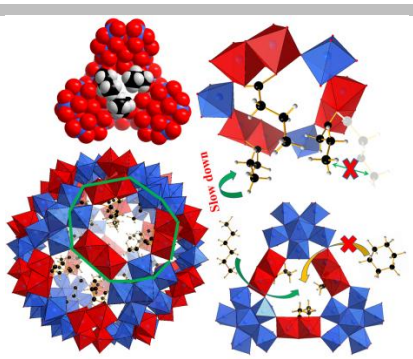

*Zhe Wang, Luke L. Daemen, Yongqiang Cheng, Eugene Mamontov, Peter V. Bonnesen, Kunlun Hong, Anibal J. Ramirez-Cuesta, and Panchao Yin**

Page No. – Page No.

Nano-Confinement inside Molecular Metal Oxide Clusters: Dynamics and Modified Encapsulation Behavior